A comparison of the tetrapyrrole cofactors in nature and their tuning by axial ligands

Jensen, Kasper P.; Rydberg, Patrik; Heimdal, Jimmy; Ryde, Ulf

Published in:
Computational modeling for homogeneous and enzymatic catalysis

2008

Document Version:
Peer reviewed version (aka post-print)

A comparison of tetrapyrrole cofactors in nature and their tuning by axial ligands

Dr. Kasper P. Jensen [a], Patrik Rydberg [b], Jimmy Heimdal [b], and Prof. Ulf Ryde [b]*

[a] Department of Chemistry, Technical University of Denmark, Building 207, Office 104, DK 2800, Lyngby, Denmark

[b] Department of Theoretical Chemistry, Lund University, Chemical Centre, P. O. Box 124, SE 221 00 Lund, Sweden

Abstract

This chapter illustrates how quantum chemical calculations can be used to elucidate structural and functional aspects of tetrapyrrole cofactors, focusing on porphyrins, cobalamins, coenzyme F430, and chlorophyll. A particular emphasis is put on the biochemical significance of axial ligands, which can tune the function of the tetrapyrroles. With the use of quantum chemical calculations, it is possible to draw important conclusions regarding aspects of tetrapyrroles that could not otherwise be accessed. The results show that the general reactivity is mainly determined by the metal and the tetrapyrrole ring system, whereas the electronic structure and reactivity are tuned by the choice of axial ligands, providing a unique insight into the design of cofactors in nature.

Keywords: haem, coenzyme B_{12}, coenzyme F430, chlorophyll, density functional theory, QM/MM

Introduction

The well-being and every-day life functions of all living creatures are determined by an overwhelming and many-faced work force of efficient catalysts, the enzymes. These molecules have evolved by random trial and error during the 3–4 billion years that life forms have existed on earth to a stage where they are so highly specialized that a small chemical change in such a molecule may cause severe disorder, disease, or even death of the affected organism.

About a third of these proteins depend either structurally or functionally on metals.[1] Two types of metals can be distinguished by their properties: main-group metals and transition metals. Both of them occur in biological systems in their ionic forms. The main-group metals, Na^+, Mg^{2+}, K^+, Ca^{2+}, and Zn^{2+}, have closed electronic configurations and occur in only one oxidation state. They have structural roles, roles as second messengers, or function as redox-inactive catalysts, e.g. Lewis acids in general acid-base chemistry. During evolution, it has become apparent that more complex tasks, including transport and storage of oxygen, containment and degradation of oxygen-based radicals, as well as electron transfer and redox reactions, have only been possible by the use of transition metals, particularly from the bio-available first row of the *d*-block. With these elements, a much more diverse chemistry can be achieved in living organisms. The transition metals occur in several oxidation states, a feature that is important for their function – they are usually redox-active.

In many cases, the metal binds directly to the protein through various amino-acid ligands. However, in other cases, some ligands are provided by a pre-arranged non-protein ligand structure, a rigid and ready-to-use catalyst module, to be incorporated into the protein. A number of similar near-planar tetradendate ligands exists in nature. They define the equatorial ligand field of an octahedral ion, leaving open two axial coordination sites. They all consist of four five-membered rings with four carbons and a nitrogen atom, similar to pyrrole and are therefore usually referred to as tetrapyrroles. The nitrogen atoms coordinate to the

central ion in all cases. The four tetrapyrrole cofactors that are the subject of this chapter are shown in Figure 1. They include coenzyme F430, cobalamin, heme, and chlorophyll.

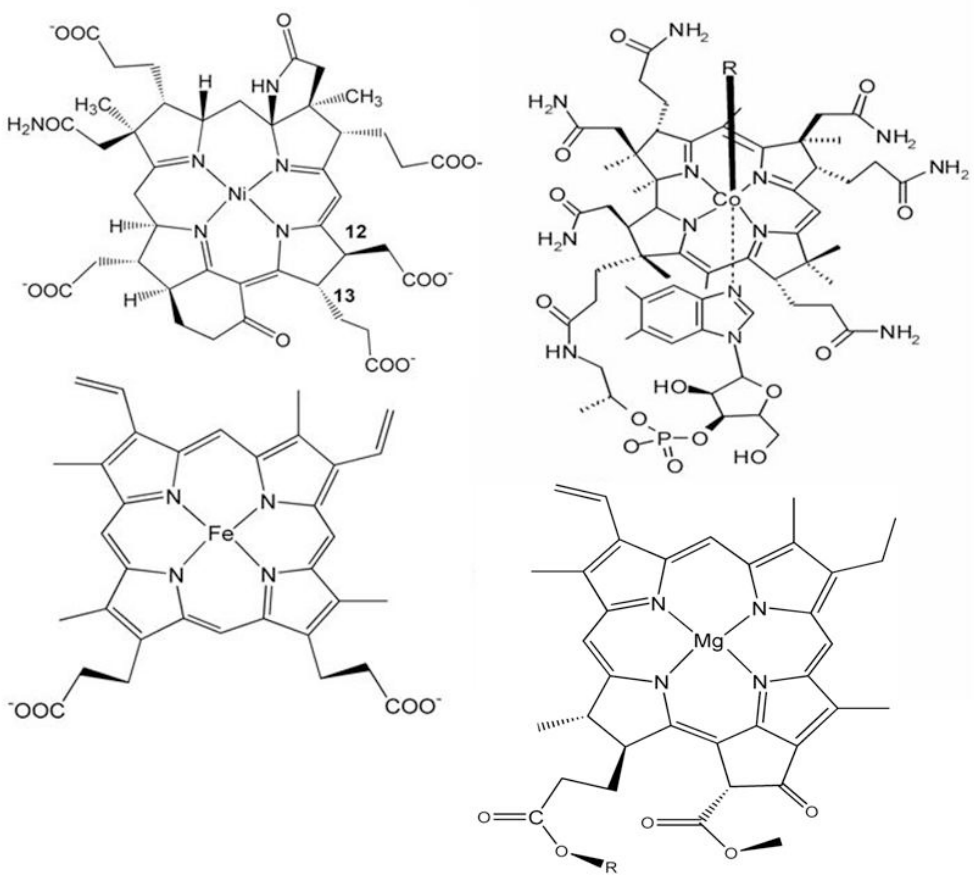

FIGURE 1. Tetrapyrrole cofactors: F430 (upper left), cobalamin (upper right), heme *b* (lower left) and chlorophyll *a* (lower right).

Tetrapyrroles are present in more than 5% of the protein structures in the protein data bank, directly implying their importance. Porphyrin is by far the most abundant (found in over 2000 structures) and diverse, in terms of function. It normally binds iron in the centre of the ring, forming the well-known heme group. Heme is used for many different functions, e.g. electron transfer in the cytochromes, binding and transport of small molecules, e.g. O_2 in the globins, and for the catalysis of a great wealth of chemical reactions, e.g. in oxidases, peroxidases, catalases, and cytochromes P450.

Chlorophylls are found in ~100 crystal structures and their prime use is as pigments in photosynthesis. They contain a Mg^{2+} ion in the centre of the tetrapyrrole ring, although the same ring system is sometimes used in nature without the metal ion, pheophytin.

The cobalamins, including coenzyme B_{12}, have a Co ion in the centre of the ring. This ion forms an organometallic Co^{III}–C bond to a methyl or a 5'-deoxyadenosyl group. The former is used in methyl transfer reactions, whereas the latter is employed in radical-based 1,2-shifts or elimination reactions.[2] Approximately 35 protein structures with cobalamin are available in the protein data bank.

Coenzyme F430, finally, is found in methanogenic archaebacteria, as part of the methylcoenzyme M reductase (MCR) complex. It contains a Ni ion, which is involved in methyl-transfer reactions.[3] It has been speculated that a Ni^{III}–C bond is formed during catalysis, in analogy with the cobalamins.[4]

The apparent similarity of the four cofactors in Figure 1 is in contrast to their widely different functions. To understand these differences, systematic studies are needed. Theoretical chemistry may play a key role in this regard, being able to answer questions that are not easily accessed by experimental means. The focus of this work is to review recent progress in understanding the similarities and differences between tetrapyrrole cofactors and how they have been designed as catalysts, with an emphasis on our own theoretical work. The first part deals with general differences between tetrapyrroles and aims at elucidating the design principles of the ring systems and the choice of the metal ions. The second part puts further emphasis on the axial ligands and how the function of tetrapyrroles has been optimized by means of particular axial ligands and their interactions with the surroundings.

Methodology

The method used almost exclusively in the reviewed work is density functional theory (DFT). The three-parameter hybrid functional B3LYP[5] achieves an impressive average absolute error of ~10 kJ/mol in relative energies of formation and 0.013 Å for bond distances for the main-group G2 test set.[6] This has made B3LYP the most widely used functional today, also within the field of inorganic chemistry.[6] With this state-of-the-art approach, reviews of many important theoretical studies of metalloproteins have been published in recent years, contributing significantly to the understanding of metalloprotein chemistry.[6,7,8,9,10,11,12]

Experience has shown that most properties, including structures, frequencies, and energies of conversions that preserve orbital occupation, can be modeled accurately with B3LYP for transition metals,[13,14] and even before the advent of hybrid functionals, successful work was carried out with generalized gradient approximation functionals,[15,16,17] such as BP86, which typically gives better geometries than B3LYP.[18] However, the energy gap between spin states is much harder to estimate and different functionals may give results that differ by over 50 kJ/mol.[19,20,21] In general, pure functionals overestimate the stability of low-spin states, whereas hybrid functionals such as B3LYP overestimate the stability of high-spin states, although to a smaller degree.[19,22] Newer functionals have been suggested with improved performance.[23,24,25,26] Moreover, it has been shown that B3LYP underestimates the bond dissociation energy (BDE) of tetrapyrrole models by favoring the open-shell dissociation products, whereas other functionals such as BP86 perform very well,[27,28] Therefore, much of this work has been performed with the BP86 functional for geometry optimization and BDEs, whereas other energies have been calculated with the B3LYP functional, consistent with the strengths of each functional.

DFT methods have successfully been applied to the study of tetrapyrroles, including both porphyrin models,[29,30,31,32,33,34,35,36,37,38,39,40,41,42,43,44,45,46,47]

cobalamin models,[27,48,49,50,51,52,53,54,55,56,57,58,59,60,61,62,63,64], F430 models,[65,66,67,68,69] and chlorophyll models.[70,71,72,73] This chapter will concentrate on work concerned with comparison of the tetrapyrrole cofactors and their tuning by the axial ligands.

Standard procedures have been used, implying optimizing geometries with double-ζ basis sets including polarization functions on heavy atoms. More accurate energies were usually calculated with a triple-ζ all-polarized basis set. Energies are usually well-converged, and only in rare cases (see below) have competing configurations been a problem during optimization of the Kohn–Sham determinant. Errors in final energies are expected to be ~20 kJ/mol for barriers, whereas relative isomerization energies are more accurate. Spin-splitting energies have larger errors, but an estimate of the error is not straight-forward. However, most functionals reproduce the correct spin state of small transition metal systems[25], so qualitatively, most conclusions in this work are expected to be valid.

We will also review perturbations caused by the axial ligands. Effects of side chains are probably small[50,74] and are not intrinsic to the cofactor in the same way, because they are affected by the surrounding protein. Thus, the molecular models applied have consisted of the bare rings – i.e. corrin (Cor), porphine (Por), hydrocorphin (Hcor), and chlorin (Chl), seen in Figure 2, combined with a variety of axial ligands.

Thus, this review is primarily directed towards comparing the *intrinsic* properties for the four metals Fe, Co, Ni, and Mg in the four tetrapyrrole ring systems Por, Cor, Hcor, and Chl, and with various sets of axial ligands. For such studies, DFT calculations in vacuum are ideal, because we want to obtain results that are not biased by differences in the surrounding proteins. However, in most cases we check the general effect of the surroundings by repeating the calculations in a continuum solvent with a dielectric constant of 4 and 80. This should illustrate possible solvation effects in any protein, because the effective dielectric constant of a protein is normally assumed to be between 2 and 20.[75] In most cases, the effect of solvation is small. However, when the reaction involves

creation or annihilation of charges, the effect may be large, e.g. for the calculation of reduction potentials and protonation reactions. Only in those cases are solvation effects discussed explicitly in this review.

In a few cases, we have gone one step further and studied reactions in specific enzymes. In those cases, we are no longer interested in the intrinsic reactivity of a site or how it compares with similar sites, but rather in the detailed energetics of a certain enzyme reaction. Then, the detailed structure of the surrounding protein is of course crucial and needs to be included. The normal way to do that is by QM/MM methods, in which the active site is treated by quantum mechanical (QM; typically DFT) methods, whereas the surrounding protein is treated by less accurate but much faster molecular mechanics (MM) methods.[76,77] Such methods normally give excellent structures, but stable and reliable energies are sometimes harder to obtain, because dynamic, entropic, and solvation effects are not properly treated.[78] We have recently developed a method to solve these problems, by performing free energy perturbations, both at the MM level and between the QM/MM and MM level, so that we can still study the interesting reaction at the DFT level. This method is called QM/MM thermodynamic cycle perturbation (QTCP).[79,80]

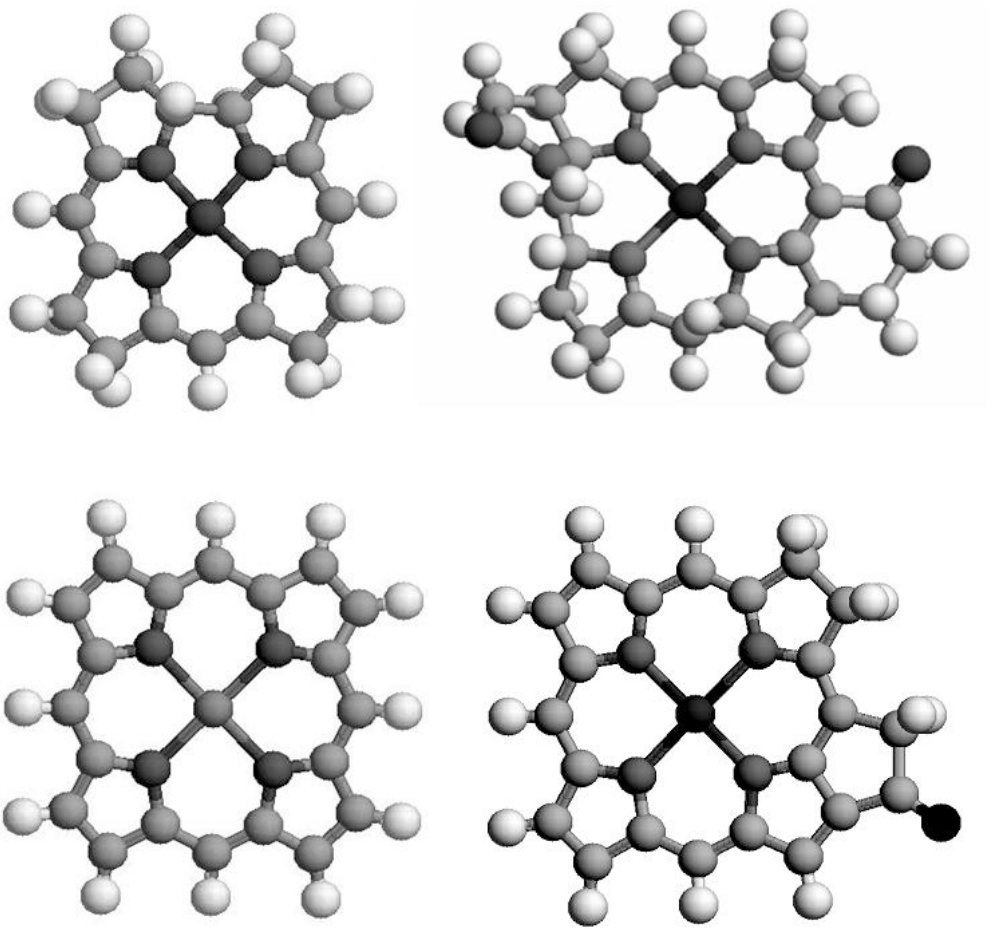

FIGURE 2. The corrin (top left), hydrocorphin (top right), porphine (bottom left), and chlorin (bottom right) rings, with Co, Ni, Fe, and Mg as central ions.

Comparison of the intrinsic chemical properties of the tetrapyrroles

Introduction

Molecular evolution is a local optimization constrained by the biochemical environment available at any given time. This is the reason why most biomolecules are astonishingly similar and belong to quite a few distinct groups of compounds.

The same situation is true for the tetrapyrrole cofactors: They differ from each other in some modest, but functionally crucial, ways. Por is most symmetric, with D_{4h} symmetry, all four rings being equivalent and the entire ring fully conjugated. Chl has one tetrapyrrole saturated and a lactone ring is fused with an adjacent pyrrole, making it a five-membered ring system. In Cor, one of the bridging methine groups is missing, and the ring is saturated on all peripheral carbons, rendering the conjugated π-system smaller. Cor has a rotation axis, giving it C_2 symmetry. Finally, the Hcor ring is completely asymmetric, with both a five-membered lactam and a six-membered lactone ring attached. The Hcor ring is even more saturated than Cor, with only five double bonds, of which two pairs are conjugated. The external rings force Hcor to be distorted, with the N–N distances differing substantially. The Por and Chl rings are dianionic, when bound to a metal, whereas Cor and Hcor are monoanions. These differences cause the cofactors to differ in the choice of metals, the number and types of preferred axial ligands, and ultimately in their function. The tetrapyrrole rings can be thought of as rigid equatorial frameworks, upon which additional functionality can be built *via* perturbations along the axis perpendicular to the ring plane.

How did the tetrapyrroles get their structures and why were these structures chosen? In the case of corrins, this matter has been discussed, but never quantified: It has been suggested that the ring cavity size is designed to fit both the Co^{III} ion and the Co^{II} ion[81] and that the Co^{II} radical in corrins may be the best way to design a directed (d_z^2) radical, which can be used reversibly during catalysis.[82] Another suggestion is that corrin has been designed as a flexible entity, which flips upwards upon response to steric strain from the lower axial ligand, transferring the strain via the corrin ring to the Co–C bond, which is thereby weakened (the so-called mechanochemical trigger mechanism).[83] Flexibility, cavity size, and orbital alignment are properties of the particular tetrapyrrole designs that can be directly probed by theoretical calculations.

Spin states

One of the most important properties of the ground state of the cofactors is the spin. In general, a transition metal can exhibit several different spin states, e.g. high spin (HS), intermediate spin (IS), and low spin (LS), depending on the number of unpaired electrons in the 3*d* orbitals, and the relative energy of these states depends on the metal and the ring system. For example, it is experimentally known[84] that iron porphyrin systems can exhibit all these spin states. On the other hand, cobalt is exclusively LS in cobalamins, in contrast to what is observed with amino-acid ligands.[85,86]

We have quantified these observations by calculating the energies of the optimized structures of the three spin states for a variety of corrins, porphyrins, and hydrocorphins with Fe, Co, and Ni in the +I, +II, and +III oxidation states.[63,66] It was found that the relative stability of the spin states was affected by both the metal and the ring system and that the two effects were approximately additive and not much affected by the axial ligand. For example, the splitting between the LS and IS states is much larger for Co^{III}Cor than for Fe^{III}Por, and the metal contributes to this difference by 40 kJ/mol and the ring system by 50 kJ/mol.[63] In general, we find that Co is always LS in tetrapyrroles. Four-coordinate Fe^{II} is IS, whereas five-coordinate complexes of Fe^{II} and Fe^{III} typically are HS and six-coordinate complexes are LS, but we will see below that all three spin states are close in energy for several of these complexes. Ni, on the other hand, is ambiguous: Four-coordinate Ni^{II} is LS, but for the five- and six-coordinate complexes of both Ni^{II} and Ni^{III}, the LS and HS states are close in energy and their relative stabilities depend both on the nature of the axial ligand and on the density functional method used (BP86 favors the LS state, whereas B3LYP favors HS). In addition, LS Ni^{II} is Jahn-Teller active and therefore normally dissociates possible axial ligands. Thus, a protein could select the HS state by providing an axial ligand, as in MCR.[66]

It is well-known that the geometries of metal complexes, in particular the bond lengths to the metal, are sensitive to the spin state:[84] The HS state gives the longest equatorial bonds, whereas those of IS and LS are similar, because only the HS state has an occupied $d_{x^2-y^2}$ orbital.[87] However, our calculations have shown that the IS states have the *longest* axial bonds, i.e. longer than those in the HS state. The reason for this is that the occupation of the $d_{x^2-y^2}$ orbital forces the iron ion out of the Por plane, which reduces the axial bond length *via* stereo-electronic effects (the equatorial Fe–N distances increases, leading to a shorter axial Fe–N bond). Thus, while the perturbations caused by the lower axial ligands affect spin, they also directly affect the geometry of the first coordination sphere.[87]

Tetrapyrroles prefer their native ions

The most direct probe into the choice of metals and tetrapyrrole rings is the energy of substituting metals among rings: Which are the most stable combinations of metal ion and ring? Are there inherent electronic or steric effects that cause some ion not to fit in some ring? Surprisingly, it was found that the native combinations of metal ions and ring systems, CoCor and FePor, are stabilized compared to the combinations FeCor and CoPor.[63] This was true for all oxidation states, I, II, and III, and for all axial ligands except one case, the six-coordinate M^{II}MeIm complexes, which are not very biologically relevant.

Even more surprisingly, the same conclusion was reached when including also combinations of Ni and Hcor.[66] When comparing Cor and Hcor, which both have a single negative charge and could be expected to be more similar choices, it was found that the native NiHcor and CoCor forms are preferred in all complexes except one, no matter the axial ligands. Altogether, these results indicate that there are strong inherent preferences of each ring for its particular metal ion, and that this is a general feature of tetrapyrrole chemistry.[66] These preferences may have been essential for the choice of the native complexes, which could then be modified to obtain a desired function, e.g. by axial perturbations.

Cavity size and flexibility of the tetrapyrroles

It has been suggested that "a fundamental difference between porphyrins, hydroporphyrins, corrins, oxoporphyrins, and other tetrapyrrole macrocycles is their optimal hole size and the range of hole sizes that are readily accessible in their complexes."[88] This is almost impossible to quantify experimentally (except indirectly by ion radii and cavity sizes), but the proposal can be addressed by computational chemistry.

Figure 3 shows the optimized potential energy surfaces for distorting the cavities of six tetrapyrroles: Por, Cor, Hcor, Chl, isobacteriochlorin (Ibc), and bacteriochlorin (Bchl).[66] The results for the first time quantized not only the cavity size, but also the *flexibility* of the ring, in terms of the energy needed to distort it. Both effects are important when discussing the design strategy of tetrapyrroles.

It is clear from Figure 3 that the cavity sizes of the various tetrapyrroles differ significantly, the order being Cor < Bchl ~ Chl < Por < Ibc < Hcor (note that Hcor has two conformational minima). The flexibility of the rings follows the trend Hcor > Cor > Por ~ Ibc > Chl > Bchl. These trends can be compared to the ionic radii of the various ions: LS Co^{III} ~ LS Fe^{III} < LS Ni^{III} < HS Ni^{III} < HS Co^{III} ~ LS Fe^{II} < HS Fe^{III} ~ LS Co^{II} < HS Ni^{II} < Mg^{2+} < HS Co^{II} < HS Fe^{II}.[89] However, these radii depend on the axial ligands and the type and charge of the equatorial ligands. Therefore, we have directly probed the ideal size of the various ring systems by using ring-broken models of the tetrapyrroles, shown in Figure 4.[63,66] These models retain the charge, the number of bonds in the chelate rings, and the conjugation of the real tetrapyrroles, but they cannot enforce suboptimal M–N distances (M is the metal) by covalent strain within the ring system.

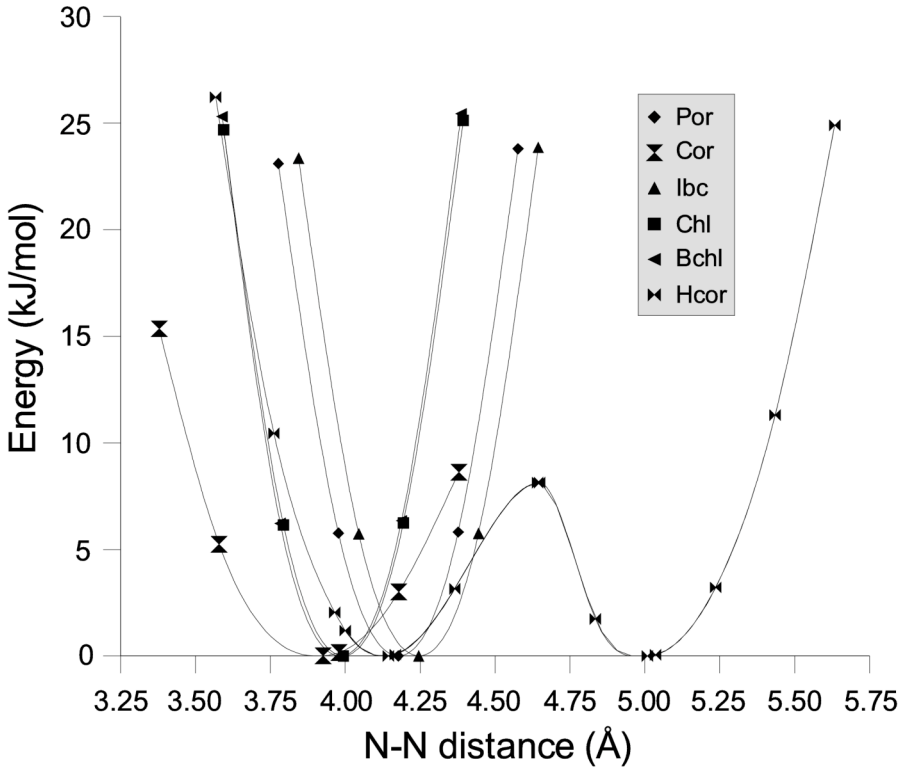

FIGURE 3. Potential energy curves for distortion of the cavities in Por, Cor, Ibc, Chl, Bchl, and Hcor.[66]

Calculations with these models showed that the cavity in Cor is ideal for LS Co^{I}, Co^{II}, and Co^{III}, because the Co–N bond lengths are the same in the normal and ring-broken models within 0.03 Å.[63,66] On the other hand, the central cavities in Por and Hcor are too large for all metals in their LS states. Thus, Hcor is ideal for incorporating the large HS Ni^{II} ion, whereas the Por ring renders also the higher spin states of Fe accessible, an effect that can be further enhanced by using the right lower axial ligand, as discussed later.

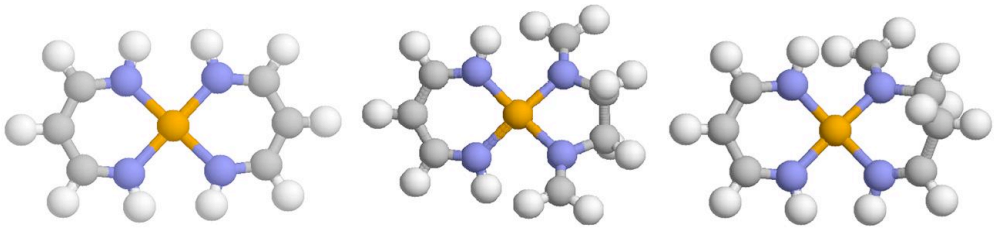

Figure 4. The three models used to estimate ring strain in Por, Cor, and Hcor, respectively.[63,66]

Cytochrome-like electron transfer

In addition to the structural preferences outlined above, a variety of functional aspects of tetrapyrroles have been compared. One important group of heme proteins is the cytochromes, whose function is to transfer electrons. According to the semi-classical Marcus equation,

$$k_{ET} = \frac{2\pi}{\hbar}\frac{H_{DA}^2}{\sqrt{4\pi\lambda RT}}\exp\left(-\frac{(E_0+\lambda)^2}{4\lambda RT}\right) \qquad (1)$$

the rate of electron transfer (k_{ET}) depends on three parameters, the electronic coupling element (H^2_{DA}), redox potential (E_0), and the reorganization energy (λ).[90] Most of these depend on the detailed structure of the proteins involved in the electron transfer. However, the inner-sphere reorganization energy, i.e. the energy difference of the electron-transfer site in the geometry of its reduced and oxidized states, is almost entirely determined by the intrinsic properties of the electron-transfer site alone, and can therefore directly be studied by quantum mechanical methods.[40]

We have calculated inner-sphere reorganization energies for a number of combinations of Fe/Co/Ni with Por/Cor/Hcor, using the most common set of axial ligands found in nature, viz. two imidazole (Im) ligands (as models of histidine).[63,66] It was found that these energies depend primarily on the type of metal. For example, the $Co^{II/III}$ pair gave reorganization energies of 179 and 197

kJ/mol in $CoPorIm_2$ and $CoCorIm_2$, respectively, whereas for the corresponding Fe complexes, the values were 8 and 9 kJ/mol, a huge difference.[63] The reason for this effect is that the d_z^2 orbital is occupied for Co^{II} (which has seven *d* electrons), but not for the other ions (which have five or six *d* electrons). This orbital is directed towards the axial ligands and therefore causes a large change of the axial bond length upon reduction of Co^{III}. Thus, octahedral cobalt complexes cannot be functional electron carriers. The Ni complexes, for which the d_z^2 orbital is occupied in both oxidation states, fall in between Co and Fe, and could in fact be decent electron carriers in tetrapyrrole complexes, in particular in Por (23 kJ/mol).[66]

The Por and Cor ring systems gave similar inner-sphere reorganization energies, and we found that they keep the reorganization energy low by restricting the change in the equatorial bonds of the metal.[40] Therefore, the more flexible Hcor ring always exhibited the largest reorganization energies with any metal ion (e.g. 23 kJ/mol for $FeHcorIm_2$). Thus, theory can explain why Fe is used as an electron carrier, but it does not explain why Por is used instead of Cor.

The reduction potential depends strongly on the surroundings, i.e. on the detailed structure of the surrounding protein. However, we can estimate the *intrinsic* potential of a certain combination of metal and tetrapyrrole ring (and axial ligands) using a continuum solvent. The resulting potentials cannot be directly compared to potentials in proteins, but they illustrate the effect of substitutions of the metals or ring systems. We have used this approach to study the reduction potential of the same complexes.[63,66] These calculations showed the trend Co < Fe < Ni for the $M^{II/III}$ couple, with differences of ~0.7 and 0.2 V. The potentials of the complexes of Por (with its double negative charge) were always lower than those of Cor and Hcor. On the other hand, we obtained the opposite trend for the I/II potentials in four-coordinated complexes: Ni < Fe < Co.[66] This confirms the stability of the Co^{I} state, which is found in corrin biochemistry, e.g.

in the mechanism of methionine synthase.[55] On the other hand, we saw no stabilization of the Ni^{I} state, which is the supposed active state of F430 in MCR.

Stability of a metal–carbon bond

Cobalamin is taken up in the body as vitamin B_{12}, but its cyano ligand is replaced with other groups to form either 5'-deoxyadenosylcobalamin (AdoCbl) or methylcobalamin (MeCbl), which are the two biologically active cofactors. Both contain a unique organometallic Co–C bond, which is cleaved during catalysis. In the case of MeCbl, the cleavage is heterolytic, with both electrons of the organometallic Co–C bond staying on cobalt to form a Co^{I} intermediate.[91] In the case of AdoCbl, the Co–C bond is cleaved homolytically, with one electron ending up in Cob(II)alamin and one in the 5'-deoxyadenosyl (Ado) radical. The Ado radical subsequently initiates a radical mechanism by which chemical groups are subject to a 1,2-shift or elimination reactions. AdoCbl is a cofactor in many enzymes, including glutamate mutase, methylmalonyl-coenzyme A mutase (MCAM), diol dehydratase, ethanolamine ammonia lyase, and class II ribonucleotide reductase. MeCbl is coenzyme in methyl transferases, such as methionine synthase (MES), corrionoid Fe/S proteins, and coenzyme M methyl transferases.[92]

Consequently, the properties of the organometallic Co–C bond have been extensively studied.[27,54,48-61] Interestingly, we found that the homolytic M^{III}–C BDE is 10 kJ/mol larger for CoCorImMe than for FePorImMe,[63] so this cannot be the reason why Co is used in these organometallic cofactors. Another idea is that the unwanted side reaction of hydrolysis is better prevented with Co–C bonds.[81] This was supported by our calculations: The Co–C bond was found to be 33–48 kJ/mol more resistant to hydrolysis than the Fe–C bond.[63]

Coenzyme F430 is also used for methyl-transfer reactions, and it has been suggested that methyl binds directly to Ni, although this has not yet been observed. Therefore, we have also studied a range of organometallic analogues of

methylcobalamin, resembling possible methylated intermediates of MCR.[66] It turned out that Ni gave the weakest M–C bonds among the three studied metals, both in the +II and +III oxidation states. In fact, the bond is so weak that suggested homolytic mechanisms of MCR[93] can be ruled out.[66,68]

We have also studied the corresponding heterolytic reactions, i.e. the transfer of a methyl group from the metal to various acceptors (e.g. a deprotonated homocysteine in MES).[63,66] Our results showed that the M–C bond strength actually follows the trend Ni < Co < Fe, with differences of 10 and 80 kJ/mol, respectively. However, the reaction energies depend strongly on the methyl donor/acceptor, and it is therefore still possible that the methyl group binds directly to Ni in MCR, provided that the donor is properly activated.[66]

Metallation reaction

The use of Mg^{2+} in chlorophyll is quite unexpected, because Mg (in variance to Fe, Co, and Ni) strongly prefers O-ligands, rather than N-donors.[85] Therefore, the binding of Mg to Chl can be expected to be less favorable than the binding of Fe to Por. In fact, it is experimentally found that the incorporation of Mg into its tetrapyrrole precursor is ATP dependent, contrary to the corresponding reaction of Fe.[94] We have compared the various reaction steps of the incorporation of Fe^{2+} and Mg^{2+} into Por with density functional methods.[95] As can be seen in Figure 5, the reaction energies are mostly quite similar and the two curves run roughly parallel. However, in the final steps of the reaction, the deprotonation of the porphyrin, there is an appreciably larger gain in energy for Fe^{2+} than for Mg^{2+}, almost 80 kJ/mol, reflecting the larger affinity of Fe^{2+} for the Por ring (before these steps, the metal ion resides above the plane of the doubly protonated ring). Moreover, the first and rate-limiting step in the reaction mechanism, the formation of the first bond between the metal and the Por ring, has a 10 kJ/mol higher activation energy with Mg^{2+} than with Fe^{2+}.

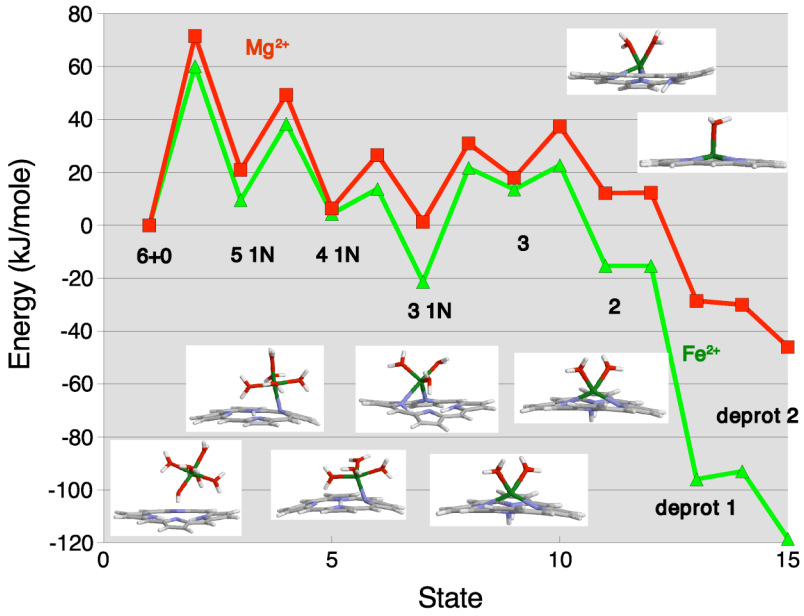

FIGURE 5. Relative energies for the various intermediates (inserted figures) and transition states for the metallation reaction of Por with Fe^{2+} (green) and Mg^{2+} (red). [95]

Tuning of tetrapyrrole structure and function by axial ligands

Introduction

After having discussed the inherent properties of the tetrapyrrole ring systems and the metals, we will now study how these properties are tuned by axial ligands. The two axial coordination sites of tetrapyrroles are distinguished as the upper side and lower side, respectively. The upper (distal or β) side is where the substrate binds. The upper site is either open for binding of solvent, substrate, or other molecules, or is it occupied by a protein ligand. The lower (proximal or α) side is occupied by an amino acid residue or a group from the cofactor itself. In heme proteins, the lower axial ligand is typically histidine (His), methionine (Met), cysteine (Cys), or tyrosine (Tyr). In cobalamins, it is His or the 5,6-dimethylbenzimidazole group at the end of one of its side chains, whereas in F430,

it is the oxygen of a glutamine (Gln) residue. In chlorophylls, many different axial ligands can be used. Thus, a great deal of variety is possible and the exact choice of lower ligand and its effect on the chemistry of the cofactor has intrigued people for decades.[96,97,98]

The importance of the lower axial ligand for B_{12} chemistry

For AdoCbl in aqueous solution, the Co–C bond is cleaved with rates of 10^{-7}–10^{-9} s^{-1} at 37° C ($\Delta G^{\ddagger}$ = 124 kJ/mol), corresponding to a half-life of ~22 years.[99,100,101] On the other hand, several coenzyme B_{12} enzymes attain catalytic rates (k_{cat}) of 2–300 s^{-1}.[102,103] Thus, the enzymes give rise to a $10^{9–13}$ fold acceleration of Co–C bond cleavage,[103,104] corresponding to a reduction of $\Delta G^{\ddagger}$ by ~70 kJ/mol. Moreover, the enzymes shift the equilibrium constant towards the homolysis products by a factor of $3 \cdot 10^{12}$ (74 kJ/mol), giving an equilibrium constant close to unity.[101,105] This cleavage initiates the subsequent radical reactions; therefore, understanding the reasons for this Co–C bond activation is arguably the most critical problem in the chemistry of B_{12}.[106]

It has long been hypothesized that the axial Co–N_{ax} bond in cobalamins is used to labilize the Co–C bond by either steric or electronic effects.[83] Until the advent of DFT methods, these questions could not be addressed directly, but the so-called mechanochemical trigger hypothesis was believed by many authors to be the most reasonable mechanism of Co–C bond activation. This hypothesis asserted that upwards butterfly folding of the corrin ring could cause strain in the Co–C bond, thus lowering the bond strength enough to provide cleavage.[83] The effect can be attenuated by the fact that the axial His ligand typically forms a hydrogen bond to the carboxylate group of a Asp residue in most structures of coenzyme B_{12} enzymes.[107,108]

The effect of the lower axial ligand has been studied by optimizing structures of B_{12}-models with a fixed Co–N_{ax} bond length.[51,53] It was found that the Co–N_{ax} bond is extremely flexible: It can be varied over a range of 0.5 Å at an

energy cost of less than 3 kJ/mol, quantifying the suggested "substantial energy cost"[109] of variations in this bond. This result explained the large variations in this bond length observed in crystal structures and also why theoretical calculations reproduced this bond length quite poorly.[51] Moreover, compression of the Co–N_{ax} bond cannot provide any significant upward folding of the corrin ring, and variations in the Co–N_{ax} bond lengths cannot change the Co–C BDE by more than a few kJ/mol (and typically the BDE is increased).[51]

In many coenzyme B_{12} enzymes, the axial His ligand forms a hydrogen bond with the carboxylate side chain of an Asp residue. We have studied the effect of the His–Asp motif, because it is known that mutation of this Asp leads to a 15–1000-fold decrease in k_{cat} of glutamate mutase.[110] We studied the extreme case in which the His ligand is deprotonated to imidazolate.[51] This led to a strengthening of the Co–N_{ax} bond and an elongation of the Co–C bond by 0.03 Å, but the BDE actually increased by 16 kJ/mol. The Co–C bond energy could be decreased by compressing the *trans* Co–N_{ax} bond, but not by more than 15 kJ/mol. This energy corresponds to a ~400-fold kinetic effect, resembling the experimental decrease in k_{cat} upon mutation of Asp.[110] The maximum of 15 kJ/mol of catalytic energy stored in the lower axial ligand is minor compared to the total $10^{9–13}$ rate enhancement[104] and not even near an explanation of the catalytic power of B_{12}-dependent enzymes.

Work by other theoretical groups[61,54] also confirmed that the effect of the axial ligand is modest. In particular, calculations of Co–C BDEs could directly probe the overstated potency of this ligand. The final conclusion from theory was that the Co–N_{ax} bond is a low-energy mode of limited catalytic importance in mutases.[51,54,61] This observation was later repeated also in a protein system, by performing QM/MM calculations of bond length distortions of AdoCbl in MCAM.[111] Instead, it has been suggested that the axial His is relevant for the discrimination between homolysis and heterolysis of the Co–C bond.[56,111]

Then how is the Co–C bond labilized? Recent QM/MM calculations[58] have helped in understanding the much debated effects of the proteins on the Co–C bond dissociation reaction. Our calculations reproduced the main experimental observations, [112,113] including an equilibrium constant between the Co^{II} and Co^{III} states close to unity, and the fact that the protein removes the barrier of bond dissociation almost completely. The amazing ability of glutamate mutase to activate the Co–C bond to the point where this step is not rate-determining was understood from the calculations as well, pointing towards a strong influence of electrostatics, both directly, via the electrostatic field, and by changing the geometry of the cofactor.[58]

It was shown by calculating the Co–C bond dissociation both with and without point charges of the protein that the direct electrostatic effect amounts to ~34 kJ/mol.[58] On the other hand, the electrostatically induced distortions of the coenzyme at short Co–C bond lengths reduced the BDE by 56 kJ/mol. However, the geometry was not changed for the lower axial ligand, as shown in Figure 6, but primarily for the polar ribose "handle" of the cofactor. In particular, the cobalt ion moved out of the corrin plane and the C–Co–N_{eq} angle was bent, in good agreement with the conformational changes that have been observed in crystallographic studies of both GluMut[114] and MCAM.[115] An extra 20 kJ/mol catalytic effect was caused by the fact that full dissociation is never accomplished in the protein, as compared to the isolated cofactor in solution.[58,116] Thus, the entire mechanism of Co–C bond labilization was explained *without* any effect of the axial His ligand.

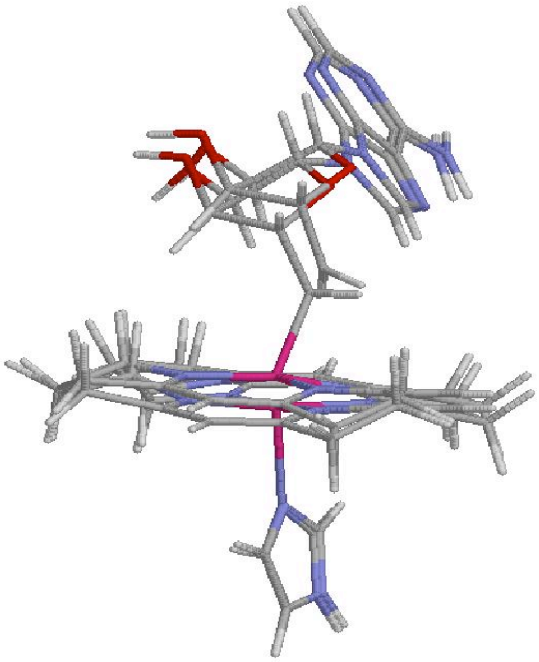

FIGURE 6. QM/MM optimized structures of the Co^{III} and Co^{II} states in glutamate mutase showing no movement of the lower axial ligand and no *trans* steric effect as the Co–C bond is broken.[58]

Recently, MCAM was studied using a similar QM/MM procedure.[117] An authentic transition state was obtained for the cleavage of the Co–C bond at a distance of 2.67 Å with an energy of 42 kJ/mol, and an intermediate was located with a modified conformation of the Ado moiety at a Co–C distance of 2.19 Å and an energy of 29 kJ/mol. It was suggested that the change in conformation of the protein and the binding of the substrate are important for the catalysis. Unfortunately, the work did not analyze how the enzyme destabilizes the Co^{III} state relative to the Co^{II} state (by ~150 kJ/mol), so the two QM/MM studies are hard to compare.

From these studies it became obvious why MeCbl cannot be used in catalysis involving homolysis of the Co–C bond: The methyl group is too small and non-polar to respond to the distortion forces.[58] The QM/MM calculated BDE for MeCbl in GluMut is only 27 kJ/mol smaller than in the isolated cofactor,

whereas for AdoCbl, the BDE is lowered by 135 kJ/mol by the protein, clearly showing this difference between the two cofactors.[58] Instead, it was found[55] that MES works by deprotonation of the methyl acceptor (homocysteine, which is bound to a zinc ion in MES[118]) and by securing a non-polar environment, which is in line with the hydrophobic environment in the crystal structure.[119] Furthermore, the Ado group cannot be subject to any nucleophilic attack, because the structure of the cofactor renders the C5′ atom inaccessible. It is notable that the axial His ligand in MES detaches during formation of the transition state.[55]

The lower axial ligand in cofactor F430

The crystal structure of MCR shows that a Gln residue binds as an axial ligand to Ni in coenzyme F430. The role of this residue may be to stabilize the HS state of Ni^{II}, which is necessary during catalysis.[120] In our calculations, we found that four-coordinate Ni^{II} Hcor complexes have a LS ground state (by 100–157 kJ/mol), whereas five-coordinate complexes with strong methyl or OH ligands preferred a HS state by 13–86 kJ/mol.[66] With weaker ligands, such as an acetamide model of Gln, the LS state is still most stable, but the Gln ligand dissociates in this state, whereas it remains bound to the metal ion in the HS states. This indicates that the enzyme deliberately selects a HS state of Ni^{II} by providing the Gln ligand.[66]

Therefore, it was concluded that the Gln residue serves as an ideal ligand for the HS Ni^{II} state: It binds weakly to the Ni^{I} state and can thus provide some guidance for changing the *d*-electron configuration upon reaction, in a manner only possible with the asymmetric structure of the Hcor ring.[66] The flexibility of the Hcor ring further adds to the cofactor's ability to deal with several large ionic states of Ni. It may be speculated that this flexibility in the ligand field of F430 is used directly during catalysis to minimize the otherwise severe effect of putting a ninth *d*-electron into an octahedral ligand field.

Importance of axial ligands for the globins

One of the classical problems of biochemistry is the binding of dioxygen to hemoglobin or myoglobin. There are several issues involved.[121] First, oxygen has to bind reversibly, i.e. with a small binding energy, and fast, i.e. with a small activation energy. The experimental binding rate is ~15 Ms^{-1},[122] but includes a multitude of sequential intermediates during the diffusion of O_2 towards the heme group. Second, O_2 is in a triplet spin state and deoxyheme is in the HS quintet state, whereas the oxyheme complex is a LS singlet. Therefore, spin crossover has to proceed.[123] We studied how globins overcome this fundamental obstacle.[41]

The ground state of oxyheme turned out to be a singlet, in accordance with experiments, with an uneven distribution of spin: It can be described as 75–80% Fe^{III}–O_2^- and 20–25% Fe^{II}–O_2. A later multiconfigurational *ab initio* study found the two configurations to be of similar weight.[124] The electronic structure is in good agreement with Mössbauer experiments,[125] where a mixture of 2/3 ferric and 1/3 ferrous forms explained the system well. Even the energy gap to the lowest triplet state agrees quite well with experiment.[126]

Next, we studied the binding of O_2 to deoxyheme for the lowest states of each spin multiplicity.[41] Interestingly, it turned out that all of them had similar energy when the Fe–O distance was more than ~2.5 Å. Such a near-degeneracy can be important for at least three reasons:[41] First, both triplet and septet states can easily lead to products (the two unpaired spins of the incoming O_2 molecule can be either parallel or antiparallel to the four unpaired electrons of deoxyheme, giving rise to these two reactant states). Second, the slope in the crossing region of the four states is small, meaning that crossing probability is large.[127] This may accelerate reversible binding by two orders of magnitude compared to non-heme FeO^+. Third, the shape of the binding curves indicates that activation energies are smaller than 15 kJ/mol, giving a rapid O_2 binding. Altogether, oxygen binding was found to be strongly accelerated and reversible, owing to the nature of the

axial ligand, which together with the intrinsic effect of the porphine ring brings spin states close in energy in ferrous heme.[41,63]

Role of axial ligands for the cytochromes

As mentioned above, the cytochromes are heme proteins whose function is to transport electrons. The cytochromes always have two axial ligands, to avoid binding of any unwanted ligands to iron. However, the axial ligands vary quite a lot, the most common combinations being two His ligands (found in most *b*-type cytochromes) or one His and one Met (found in most *c*-type cytochromes).[85]

We have calculated inner-sphere reorganization energies of cytochrome models with seven different combinations of axial ligands.[40] The results (Table 1) showed that neutral axial ligands (His, Met, and a neutral amino terminal) give a low inner-sphere reorganization energy, 5–9 kJ/mol. However, if one of the axial ligands is negatively charged (Cys, Tyr, or Glu), the reorganization energy is appreciably larger, 20–47 kJ/mol. Interestingly, such charged ligands are typically used only if the heme site also has other functions than electron transfer (e.g. catalysis). This illustrates the importance of the inner-sphere reorganization energy in electron transfer and it also explains the choice of axial ligands for the cytochromes.

Still, it should also be noted that even the reorganization energies with the charged ligands are quite low. In fact, the inner-sphere reorganization energies of the cytochromes are appreciably lower than those of the other two important groups of electron carriers found in nature, viz. the blue copper proteins and the iron-sulfur clusters (43–90 kJ/mol and 40–75 kJ/mol, respectively).[40,128,129,130,131] The reason for this is that the preferred geometry of Fe^{II} and Fe^{III} in the octahedral field of the cytochromes is very similar, and that the small difference in the preferred Fe–ligand distances is reduced by covalent strain in the rigid porphyrin unit by ~0.05 Å, leading to a decrease in the reorganization energy of ~8 kJ/mol. It is also important that both oxidation states of Fe are in the LS state – in the HS

state, the reorganization energy would be 20–30 kJ/mol higher, owing to the longer Fe–N bond lengths. Finally, the compensation of two charges in the porphyrin ring and the delocalization of the charge over the rather soft N and S ligands are also important for the low reorganization energy in the cytochromes.[40]

TABLE 1. Inner-sphere reorganization energies[40] and reduction potentials for seven cytochrome models. Amt is a neutral amino terminal.

Axial ligands		Reorganization	Reduction potential (V)		
1	2	energy (kJ/mol)	ε=1	ε=4	ε=80
Met	Met	4.8	1.41	0.53	0.12
His	Met	8.3	0.57	-0.25	-0.63
His	His	8.2	0.39	-0.38	-0.72
His	Amt	8.6	0.45	-0.42	-0.82
His	Cys	20.0	-3.51	-2.23	-1.56
His	Tyr	47.0	-3.24	-2.16	-1.62
His	Glu	26.4	-3.11	-1.97	-1.40

We have also studied the reduction potential, calculated in continuum solvents with different values of the dielectric constant (ε), ranging from 1 (vacuum) to 80 (water). The results of such calculations[40] are also shown in Table 1. It can be seen that the reduction potentials are much more sensitive to the choice of the axial ligands than the reorganization energies. Thus, the cytochromes can fine-tune their reduction potentials by the choice of axial ligands, without changing the reorganization energies significantly. The redox potentials strongly depend on the value of the dielectric constant. However, the relative potentials of different sets of ligands are fairly constant (at least for the neutral ligands). For example, the His–Met set gives a 0.10–0.17 V higher potential than the His–His set, which is in fair accordance with the experimental difference of 0.17–0.30 V for these two sets of ligands in actual proteins.[85,132] The Met–Met set causes an even higher

potential, whereas the His–amino-terminal set provides a potential similar to that of the His–His set. Thus, our results indicate that the axial ligand is used by the cytochromes to tune the reduction potential, rather than the reorganization energy.

Role of the axial ligand in heme enzymes

As mentioned above, the heme group is used in many different heme proteins. We have already discussed two important groups, viz. the globins and the cytochromes. A third important and diverse group are the oxidizing heme enzymes, including heme peroxidases, catalases, and cytochromes P450. All heme enzymes contain only one axial ligand from the protein, leaving the sixth coordination site free for the binding of a substrate. However, this axial ligand differs between the various types of heme enzymes: The cytochromes P450, as well as chloroperoxidase and NO synthase, have a Cys ligand, whereas all heme peroxidases use a His ligand, and all heme catalases utilize a Tyr ligand. Both the Cys and the Tyr ligands are expected to bind in their deprotonated, negatively charged forms.

Moreover, the properties of the axial ligand are tuned by its interactions with second-sphere ligands. Thus, the His ligand in the heme peroxidases invariably forms a hydrogen bond to the carboxylate group of an Asp residue, similar to the His ligand in the coenzyme B_{12} enzymes (Figure 7). This is in variance with the globins, which do not possess such a hydrogen bond. Likewise, the Tyr ligand in the catalases invariably forms a hydrogen bond to the positively charged side chain of an Arg residue (Figure 7), and the Cys ligand in NO synthase forms a hydrogen bond with a tryptophane residue.[133] It is likely that these hydrogen-bond interactions may tune the properties of these groups, so they were also included in the theoretical studies.

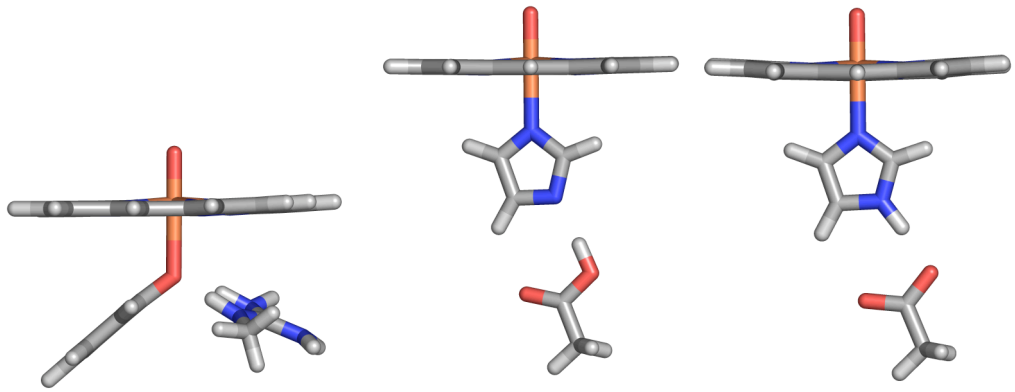

FIGURE 7. Three models with second-sphere hydrogen bonds (all showing compound I): Tyr+Arg (left) and His+Asp, with the proton either on Asp (middle, His+HAsp) or on His (right, HisH+Asp).

Heme peroxidase, catalase, and cytochrome P450 are involved in similar catalytic cycles, as illustrated in Figure 8. The resting state of cytochrome P450 is the Fe^{III} state with a water molecule bound to Fe. When the enzyme binds the substrate, the water molecule is displaced and the spin state changes to HS. After reduction to Fe^{II}, O_2 binds to heme (note that these are the only two states used by the globins). After another reduction, a proton is bound, forming a Fe^{III}-hydroperoxide complex. This complex takes up another proton, which triggers the cleavage of the O–O bond and the formation of a highly reactive state, called compound I, which formally is a Fe^{V}–O^{2-} complex. It can oxidize almost any compound, by hydrogen abstraction (and rebound of the formed radical to a hydroxide compound), epoxidation, or N, S, or SO oxidation. The intermediate after hydrogen abstraction is a Fe^{IV}–OH^{-} complex, whereas the product after the full reaction is the resting Fe^{III} state, possibly with the product, rather than a water molecule bound.

On the other hand, the heme peroxidases bind hydrogen peroxide, which after deprotonation and reprotonation on the terminal oxygen forms compound I. However, in this class of enzymes, the active site is not large enough to bind a substrate larger than hydrogen peroxide. Instead, the substrates bind on the

surface of the protein and are oxidized by one-electron transfer from the heme site, which first forms a $Fe^{IV}O$ state, called compound II, and then the Fe^{III} resting state after a second electron transfer. The reaction mechanism for catalases is identical up to the formation of compound I. However, this intermediate then reacts with another hydrogen peroxide molecule to form O_2. Thus, the catalases catalyze the disproportionation of two H_2O_2 molecules to water and O_2.

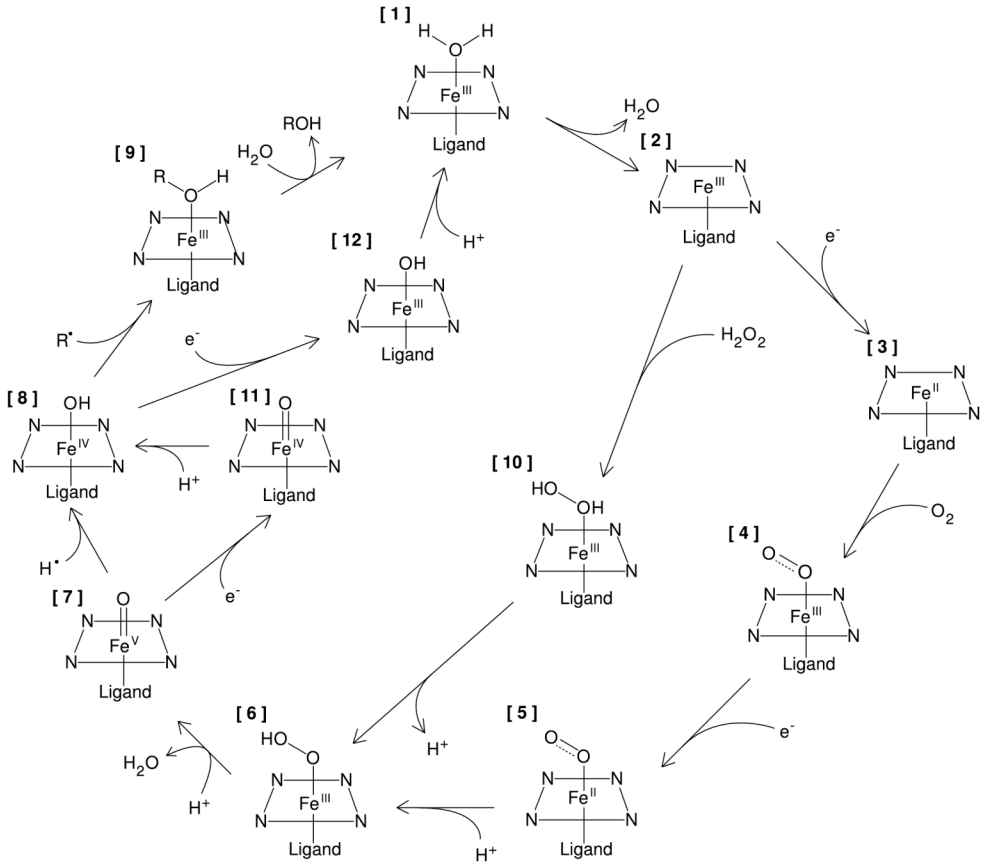

FIGURE 8. The reactions involved in the cycles of cytochrome P–450 (states 1-9), peroxidase (states 1, 2, 10, 6, 7, and 8 or 11), and catalase (states 1, 2, 10, 6, and 7).

We have studied the influence of axial ligands for all the twelve reaction intermediates in Figure 8, using five different sets of axial ligands: His, His+Asp,

Cys, Tyr, and Tyr+Arg.[47] Naturally, the five types of axial ligands display extensive variation in their distances to the Fe ion. In general, the bond lengths follow the trend Tyr < Tyr+Arg ≈ His+HAsp < HisH+Asp < His < Cys. On the other hand, the Fe–O distances on the distal side follow the trend: His < Tyr+Arg < HisH+Asp < His+HAsp ≈ Tyr < Cys.

More interesting than these structural differences are their effect on the reaction energies. We have studied how the axial ligand influences all the reactions shown in Figure 8.[47] For most reactions, the energies follow the trend Cys < Tyr < Tyr+Arg < His+Asp < His, reflecting the donor capacity of the various ligands. The most pronounced effects are seen for the reduction potentials. In particular, the $Fe^{II/III}$ reduction potential is negative and increases in solution for the negatively charged ligands (Tyr, Cys, and His+Asp), whereas it is more positive and decreases in solution for the two neutral ligands (His and Tyr+Arg). This is in agreement with the experimental potentials of catalase (<–0.5 V), cytochrome P450 (–0.30 V), horseradish peroxidase (–0.22 V), and myoglobin (+0.05 V).[47] Thus, the choice of a neutral His ligand in the globins is important to avoid the formation of the inactive Fe^{III} form.

Even more important are the next two steps of the reaction, the reduction and protonation of the O_2 complex, which appear to be concerted according to the calculations: The reduction potential is 0.3–0.4 V more negative for His than for the other four ligands, indicating that it is appreciably harder to reduce the Fe^{II}–O_2 complex in the globins (an unwanted side-reaction) than in the other enzymes (an essential step for cytochrome P450).

The reduction potential of the compound I/II couple exhibits a similar trend: Tyr < Cys < Tyr+Arg < His+Asp < His. This is also functionally appropriate: The potential in cytochrome P450 and catalase should be as negative as possible to avoid the formation of compound II, whereas for the peroxidases, the reduction potentials of compound I and II should be as similar as possible, because the two states should oxidize the same substrate. Experimentally, the

reduction potentials are 0.90 and 0.87 V for horseradish peroxidase[134]. In the calculations, we obtain a 0.1–0.3 V lower potential for compound II with any type of ligand.

Moreover, there is a pronounced effect of the negative axial ligands (but not of Tyr+Arg) on the formation of compound I in a hydrophobic environment: the reaction from the hydroperoxide complex is 80–140 kJ/mol more exothermic for Cys, Tyr, and His+Asp than for His in a continuum solvent with $\varepsilon = 4$. This effect of the negatively charged axial ligand has often been termed a push effect.[135] However, the effect strongly depends on solvation and disappears in a water-like continuum solvent.

Finally, we observed that the Tyr and Tyr+Arg ligands cause a 8–20 kJ/mol more exothermic reaction energy for the reaction of H_2O_2 with compound I than the other three ligands do. This is relevant for the second step of the catalase reaction cycle, indicating that the choice of the Tyr ligand is also appropriate in this case.

On the other hand, calculations did not reveal any effect of the axial ligand on the O_2 affinity or the hydrogen-atom abstraction. Likewise, there was no indication that negatively charged ligands should favor a heterolytic, rather than a hemolytic, splitting of O–O, and we even found an opposite effect for the P450 oxidation step, i.e. that the His model gives a more favorable energy than the Cys model.[47] More recent studies have compared the activation energies for hydrogen abstraction using models with Cys, His, and Tyr ligands, but found small differences, sometimes indicating a lower barrier for His than for Cys.[136,137] In particular, His models seem to prefer epoxidation, whereas Cys models favor hydrogen abstraction. For sulfoxidation, there is no difference between Cys and His, in terms of activation barriers.[138]

Tuning the His ligand by hydrogen bonds in heme proteins

We have seen that the axial His ligand in both heme peroxidases and coenzyme B_{12} enzymes is hydrogen bonded (by the non-coordinating N atom of the imidazole ring) to a carboxylate group (Figure 9) and that this may influence its properties. We have therefore studied this interaction in more detail and compared it to the limiting cases of no carboxylate group or a fully deprotonated imidazolate group, as well as to a case with a weaker hydrogen bond to a carbonyl group, encountered in the cytochromes and globins.[87]

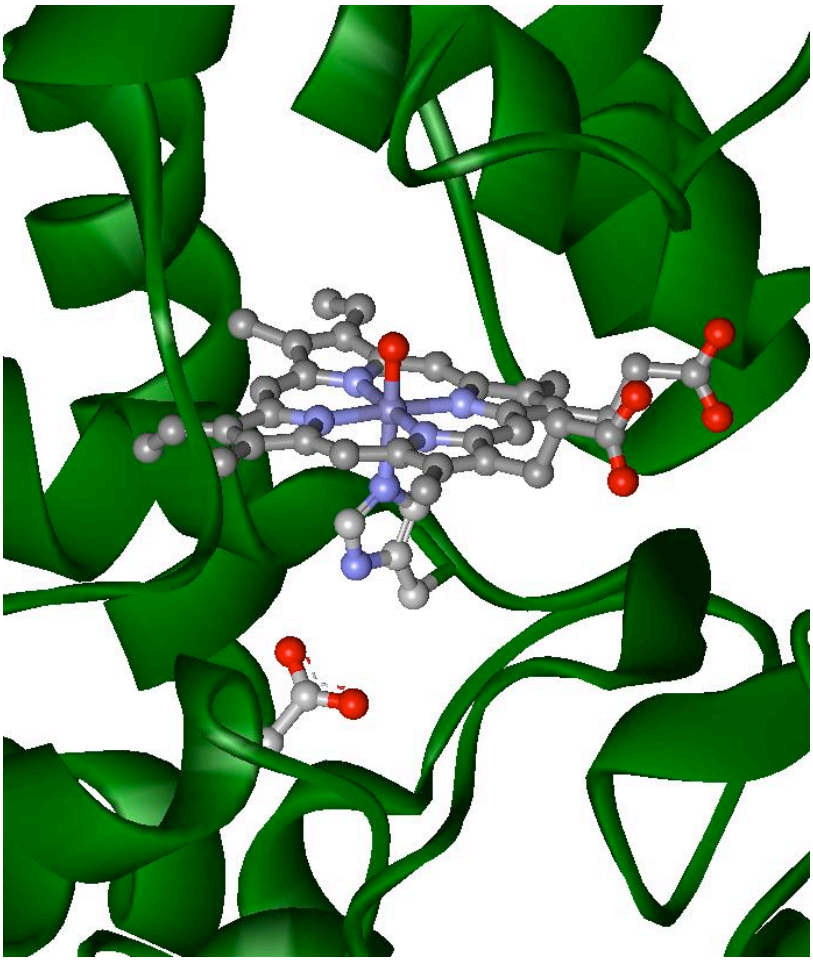

FIGURE 9. The arrangement of the amino acids His and Asp on the proximal side of heme in compound I of horseradish peroxidase.[139]

The results showed that a hydrogen bond to a carbonyl group had a small influence on the geometry and properties of the heme site. On the other hand, hydrogen bonds to a carboxylate group could have a large influence, especially if the proton shared in this hydrogen bond moved to the carboxylate group.

It was also found that the spin splitting energy of the Fe^{II} heme states with neutral imidazole resembles those of Fe^{III} heme states with imidazolate, i.e. all spin states came close in energy.[87] We have seen that such degeneracy is important for the rapid binding of O_2 to the globins.[41] The interesting thing is that heme peroxidases bind the H_2O_2 substrate in the Fe^{III} state (cf. Figure 8), which requires a spin conversion similar to that in the globins. Thus, the choice of the His+Asp ligand may be a means to facilitate binding of small molecules to the heme group. These studies together put a new emphasis on the choice of axial ligand in heme proteins, a subject of very intense debate during the last 20 years.[140,141]

On the other hand, the inner-sphere reorganization energies were not affected significantly by the perturbations, which indicates that proximal hydrogen bond networks can be used to tune redox potentials in heme groups without increasing reorganization energies.[87]

Recently, a detailed QM and QM/MM study was presented of how various proximal and distal perturbations affect the O_2 affinity of Fe^{II}PorIm heme sites.[142] They studied the effect of rotations of the His ligand, the distance of the His ligand to the heme plane, as well as three different types of hydrogen bonds to the His ligand (His–carbonyl, His–Asp+Tyr, and His–H_2O–back-bone NH) and two actual proteins (myoglobin and leghemoglobin). Changes in the O_2 affinity were observed, of up to 15 and 30 kJ/mol for proximal and distal perturbations, respectively.

Considering the importance of the location of the shared proton in heme peroxidase, i.e. whether the proton resides on Asp (His+HAsp, Figure 7 mid, giving a deprotonated imidazolate group) or on His (HisH+Asp; Figure 7 right),

we have used several different methods to determine its position in various states of the reaction mechanism.[143] First, we investigated the relative stability of the two protonation states in vacuum, using the small FePorImAc model (Ac=acetate) and various upper ligands. It turned out that for most complexes, the HisH+Asp state is more stable, although the energy difference was small (1–2 kJ/mol), except for the reduced O_2 complex (37 kJ/mol). However, for the five-coordinate complex without any ligand, and for compound II, the His+HAsp state was more stable (by 18–37 kJ/mol). Yet, these energies strongly depended on the solvation effect, and in a water-like continuum solvent, the HisH+Asp state was stabilized, rendering it the ground state for all complexes, except in the case of the five-coordinated complex.

Interestingly, these results also depend on the nature of the computational porphyrin model. For the HS $Fe^{III}H_2O$ state, the truncated Por model without any side chains indicated that the His+HAsp state is more stable by 10 kJ/mol, whereas a model with all the porphyrin side chains indicated that the HisH+Asp state is 2 kJ/mol more stable. This is the only time that we have found a significant effect of the side chains.

Next, we studied the stability of the two states with QM/MM methods. They indicated that the HisH+Asp state is more stable for all six complexes studied (by 4–64 kJ/mol). However, QM/MM studies often do not treat solvation effects properly and may therefore overestimate electrostatic interactions. Therefore, we also studied the energy difference between the two protonation states using the QTCP[79,80] method.[143] As expected, this reduced the energy difference, but still the HisH+Asp state was more stable (by 12–50 kJ/mol) for all states, except the $Fe^{IV}OH$ model, for which the two states were degenerate within 4 kJ/mol.

Finally, we re-refined a crystal structure of cytochrome *c* peroxidase in the resting $Fe^{III}H_2O$ state,[144] using the quantum refinement procedure,[145,146] i.e. standard crystallographic refinement where the molecular mechanics potential

used to supplement the experimental data is replaced by QM calculations for the heme site.[143] Unfortunately, the results were not conclusive: The HisH+Asp state gave slightly lower crystallographic *R* factors (0.18669 compared to 0.18673), but the His+HAsp state gave a 1–9 kJ/mol lower strain energy (i.e. the energy difference of the quantum system optimized in vacuum or in the crystal structure) and better electron density difference maps. Because of this, we concluded that in the Fe^{III} resting form, the two protonation states are close in energy, whereas in all other catalytically significant states of the peroxidase reaction cycle, the HisH+Asp state is more stable.

The axial ligand in chlorophylls

The Mg^{2+} ion in chlorophyll typically binds one additional axial ligand, but this ligand varies substantially. A survey of three crystal structures with a total of 308 chlorophylls showed that the most common ligands are His and water, but Asp/Glu, Tyr, methionine (Met), serine (Ser), asparagine/glutamine (Asn/Gln), and the back-bone amide groups are also observed, as well as phosphate and alcohol groups from non-protein molecules.[44] Fourteen of the chlorophylls do not have any fifth ligand, and none is six-coordinate.

In line with earlier work, we studied the influence of the axial ligand on the properties of the Chl and Bchl molecules, using 11 different models of axial ligands.[44] The Mg–ligand bond length was 1.90–1.99 Å for the negatively charged ligands (Ser^- < Asp < and phosphate), 2.10–2.21 Å for most neutral ligands (backbone < Asn < Ser < H_2O < Tyr < His), and even longer with two His ligands (2.35 Å) or with Met (2.74 Å).

The Mg–ligand bond length reflects the bond strength quite well: The BDE of the various axial bonds are 28–70 kJ/mol for the neutral and 170–260 kJ/mol for the negatively charged ligands, and they follow the same trends as the bond lengths, with the single exception that His gives the strongest bond among the neutral ligands.[44] Such bond energies are similar to what is found for other

tetrapyrroles. However, the binding of a second axial ligand to Chl is unusually weak. In fact, there is no gain in energy of a second His ligand to Chl in a continuum solvent. In contrast, the corresponding energies for Fe^{II}PorIm are 23–51 kJ/mol. This explains why chlorophyll almost invariably is five-coordinate in crystal structures (four-coordinate structures are almost only observed in low-resolution crystals, where no water positions are reported[44]). This also casts some doubt on most previous theoretical studies of Chl, which were performed on four-coordinate models. In fact, it has been noted that the calculated properties of Chl models are improved if a fifth ligand is included in the calculations.[147]

The prime use of chlorophylls in nature is as pigments for the harvesting of light energy in photosynthesis. Therefore, we also studied the effect of axial ligands on the absorption spectra of chlorophylls.[44] The spectra were calculated with time-dependent DFT using the BP86 functional. In general, the absorption wavelength of both the Q and B bands (the major absorption bands around 660 and 430 nm for chlorophyll *a*) was increased by axial ligands. For the B band, the shift was 6–14 nm for the neutral ligands and 28–35 nm for the negatively charged ligands. For the Q band, the shift was half as much.[44] In the case of Bchl, the changes were somewhat smaller and negative for the Q band. Thus, the axial ligands can fine-tune the absorption properties of the chlorophylls, but the effect is quite restricted. In particular, axial ligands cannot alone explain the so-called red chlorophylls in photosystem I, which display spectral shifts of up to 50 nm.[148] This indicates that the protein surroundings and the possible formation of chlorophyll multimers are at least as important as the axial ligands for the absorption properties of the chlorophylls.

Furthermore, the effect of axial ligands on the reduction potentials of the chlorophylls was investigated,[44] because chlorophylls are also involved in the electron transfer paths of the photosynthetic reaction centers. It was found that the axial ligands have quite strong effects on the potentials of chlorophyll, both for its reduction and its oxidation. Both potentials decreased, by 0.1–0.5 V for the

neutral ligands, and by up to 3 V for the charged ligands in vacuum, following approximately the same trends as the Mg–ligand bond lengths. However, the effect is strongly diminished if solvation effects are included, and in a water-like continuum solvent, the reduction potentials of all models were the same within 0.2 V. However, the potentials are still 0.1–0.2 V lower than Chl without any axial ligand. Pheophytin was predicted to have a potential 0.2 V higher than the four-coordinate chlorophyll. Thus, it could be concluded, in line with the cytochrome work, that the axial ligands can be used to fine-tune the reduction potentials of the chlorophylls.

Interestingly, such tuning seems to occur in many proteins. In photosystem I, the electron-transfer path consists of the reaction centre P700 (a special chlorophyll dimer), a chlorophyll molecule ligated by water, followed by a chlorophyll ligated by Met.[149] According to our calculations, the reduction potential of a neutral Chl model is more negative if the axial ligand is water than if it is Met (–1.87 and –1.79 V in a protein-like continuum solvent).[44] This means that the electron transport from the chlorophyll ligated by water to that ligated by Met is favorable. It has been proposed that this is a mechanism to prevent back-transfer of the electrons.[150] Interestingly, a similar arrangement is observed both in photosystem II and the bacterial reaction center, i.e. the second electron acceptor has a more negative potential than the third one (although the molecules and ligands are different),[44] indicating that this may be a general mechanism.

Concluding remarks

In this chapter, we have reviewed our computational efforts to understand why nature has selected certain combinations of metals, tetrapyrrole ring systems, and axial ligands in different proteins. Traditionally, biochemical investigations are performed by experimental methods, but we have seen that such hypothetical questions are appropriate to study with computational methods instead. With these methods, we obtain pure results about intrinsic differences, which are not

biased by differences in the surrounding proteins or by the possibility of conformational changes in mutational studies, for example. Moreover, we can perform computational experiments that are hard and time consuming to perform in a lab.

These studies have pinpointed many important reasons for nature's choice of various metals, tetrapyrroles, and axial ligands:

- Corrin has the smallest central cavity, which fits ideally low-spin Co in all three relevant oxidation states (+I, +II, and +III).
- Porphyrin is selected to allow iron chemistry in both high-spin (substrate free) and low-spin state (with substrate bound). Its double negative charge has a strong influence on the reduction potentials, stabilizing the +IV and +V formal oxidation states, but making the +I state unavailable.
- The hydrocorphin ring has a larger central cavity and is more flexible than the other ring systems. Therefore, it fits the large Ni^{II} ion and the Ni^{I} ion with its singly occupied $d_{x^2-y^2}$ orbital.
- The $Fe^{II/III}$ couple is ideal for electron transfer in the cytochromes, giving a minimal reorganization energy, because the redox-active orbital is not directed towards any ligand.
- Co^{III} provides an ideal Co–C bond that is of intermediate strength, strong enough to resist hydrolysis, but weak enough so that it can be readily broken in enzymes by both homolytic and heterolytic pathways.
- Mg^{2+} is an unexpected metal in tetrapyrrole chemistry. Its incorporation into a tetrapyrrole has a higher activation energy and a less favorable reaction energy than for Fe^{2+}.
- Neutral axial ligands have a small influence on the reorganization energies, but they can tune the redox potentials.

- Negatively charged axial ligands have a strong influence on the properties of heme sites, affecting both the redox potential and reaction energies, and therefore playing an important role in determining the reactivity of heme enzymes.
- The effect of axial ligands can be tuned by hydrogen bonds to nearby residues, especially if the latter are charged.
- The axial heme ligand affects the spin-splitting energies, a feature used by both globins and peroxidases to facilitate the spin-forbidden binding of substrates.
- The axial ligand of coenzyme B_{12} enzymes has a smaller influence on the reactions than previously supposed (but not smaller than the average effect of axial ligands in heme enzymes). Instead, the surrounding enzyme has a major influence on these reactions.
- The Gln ligand of coenzyme F430 is an ideal weak ligand, indifferent for the Ni^{I} state, but enforcing a high-spin state for Ni^{II}.
- Chlorophyll can only bind one axial ligand, in variance to the other tetrapyrroles. This ligand can tune the absorption properties and reduction potentials of these sites in a functional way.

In conclusion, we have seen that in most cases there is a rationale behind the choices of metals, tetrapyrroles, and axial ligands for nature's design of cofactors, and that this rationale has been partly uncovered by theoretical calculations.

Acknowledgements

This investigation has been supported by funding from the research school in medicinal chemistry at Lund University (FLÄK) and the Swedish research council (VR). It has also been supported by computer resources of Lunarc at Lund University.

References

[1] D. Ghosh, V. L. Pecoraro, *Curr. Opin. Chem. Biol*. **2005**, *9*, 97.
[2] M. L. Ludwig, R. G. Matthews, *Annu. Rev. Biochem*. **1997**, *66*, 269.
[3] M. A. Halcrow, G. Christou, *Chem. Rev.* **1994**, *94*, 2421.
[4] U. Ermler, W. Grabarse, S. Shima, M. Goubeaud, R. K. Thauer, *Science* **1997**, *278*, 1457.
[5] A. D. Becke, *J. Chem. Phys*. **1993**, *98*, 5648.
[6] P. E. M. Siegbahn, *J. Biol. Inorg. Chem*. **2006**, *11*, 695.
[7] L. Noodleman, T. Lovell, W.-G. Han, J. Li, F. Himo, *Chem. Rev*. **2004,** *104*, 459.
[8] M.-H. Baik, M. Newcomb, R. A. Friesner, S. Lippard, *Chem. Rev*. **2003**, *103*, 2385.
[9] F. Himo, P. E. M. Siegbahn, *Chem. Rev*. **2003**, *103*, 2421.
[10] S. Shaik, D. Kumar, S. P. de Visser, A. Altun, W. Thiel, *Chem. Rev*. **2005**, *105*, 2279.
[11] T. A. Jackson, T. C. Brunold, *Acc. Chem. Res*. **2004**, *37*, 461.
[12] G. H. Loew, D. L. Harris, *Chem. Rev*. **2000**, *100*, 407.
[13] G. Frenking, N. Frohlich, *Chem. Rev*. **2000**, *100*, 717.
[14] P. E. M. Siegbahn, M. R. A. Blomberg, *Chem. Rev*. **2000**, *100*, 421.
[15] T. Ziegler, *Chem. Rev*. **1991**, *91*, 651.
[16] T. Ziegler, *Can. J. Chem*. **1995**, *73*, 743.
[17] P. E. M. Siegbahn, M. R. A. Blomberg, *Annu. Rev. Phys. Chem*. **1999**, *50*, 221.
[18] U. Ryde, *Dalton Transact.* **2007**, 607-625.
[19] F. Neese, *J. Biol. Inorg. Chem*. **2006**, *11*, 702.
[20] J. F. Harrison, *Chem. Rev*. **2000**, *100*, 679.
[21] J. Li, G. Schreckenbach, T. Ziegler, *J. Am. Chem. Soc*. **1995**, *117*, 486.
[22] M. Swart, A. R. Groenhof, A. W. Ehlers, K. Lammertsma, *J. Phys. Chem. A* **2004**, *108*, 5479-5483.
[23] Y. Zhao, N. E. Schultz, D. G. Truhlar, *J. Chem. Phys.* **2005**, *123*, 161103.
[24] N. E. Schultz, Y. Zhao, D. G. Truhlar, *J. Phys. Chem. A* **2005**, *109*, 11127.
[25] K. P. Jensen, B. O. Roos, U. Ryde, *J. Chem. Phys.* **2007**, *126*, 014103.
[26] A. Fougueau, S. Mer, M. E. Casida, L. M. L. Daku, A. Hauser, F. Neese*, J. Chem. Phys*. **2005**, *122*, 044110.
[27] K. P. Jensen, U. Ryde, *J. Phys. Chem. A* **2003**, *107*, 7539.
[28] J. Kuta, S. Patchkovskii, M. Z. Zgierski, P. M. Kozlowski, *J. Comput. Chem*. **2006**, *27*, 1429.
[29] A. Ghosh, *J. Am. Chem. Soc*. **1995**, *117*, 4691.
[30] A. Ghosh, *Acc. Chem. Res*. **1998**, *31*, 189.
[31] A. Ghosh, E. Gonzalez, T. Vangberg, *J. Phys. Chem. B* **1999**, *103*, 1363.
[32] T. G. Spiro, P. M. Kozlowski, M. Z. Zgierski, *J. Raman Spectr.* **1998**, *29*, 869.
[33] P. M. Kozlowski, T. G. Spiro, A. Bérces, M. Z. Zgierski, *J. Phys. Chem. B* **1998**, *102*, 2603.
[34] M. Wirstam, M. R. A. Blomberg, P.E.M. Siegbahn, *J. Am. Chem. Soc*. **1999**, *121*, 10178.
[35] M. R. A. Blomberg, P. E. M. Siegbahn, G. T. Babcock and M. Wikström, *J. Inorg. Biochemistry* **2000**, *80*, 261.
[36] P. E. M. Siegbahn, *J. Comput. Chem*. **2001**, *22*, 1634.
[37] D. L. Harris, G. H. Loew, *J. Am. Chem. Soc*. **1998**, *120*, 8941.
[38] C. Rovira, K. Kunc, J. Hutter, P. Ballone, M. Parinello, *J. Phys. Chem. A* **1997**, *101*, 8914.
[39] F. Ogliaro, S. Cohen, S. P. de Visser, S. Shaik, *J. Am. Chem. Soc.* **2000**, *122*, 12892.
[40] E. Sigfridsson, M. H. M. Olsson, U. Ryde, *J. Phys. Chem. B* **2001**, *105*, 5546.
[41] K. P. Jensen, U. Ryde, *J. Biol. Chem*. **2004**, *279*, 14561.
[42] B. van Oort, E. Tangen, A. Ghosh, *Eur. J. Inorg. Chem*. **2004**, 2442.
[43] M. P. Johansson, M. R. A. Blomberg, D. Sundholm, M. Wikstrom, *Biochim. Biophys. Acta* **2002**, *1553*, 183.
[44] J. Heimdal, K. P. Jensen, A. Devarajan, U. Ryde, *J. Biol. Inorg. Chem.* **2007**, *12*, 49.

[45] H.-P. Hersleth, U. Ryde, P. Rydberg, C. H. Görbitz & K. K. Andersson, *J. Inorg. Biochem*. **2006**, *100*, 460.
[46] E. S. Ryabova, P. Rydberg, M. Kolberg, E. Harbitz, A.-L. Barra, U. Ryde, K. K. Andersson, E. Nordlander, *J. Inorg. Biochem*. **2005**, *99*, 852.
[47] P. Rydberg, E. Sigfridsson, U. Ryde, *J. Biol. Inorg. Chem*. **2004**, *9*, 203.
[48] T. Andruniow, M. Z. Zgierski, P. M. Kozlowski, *J. Phys. Chem. B* **2000**, *104*, 10921.
[49] T. Andruniow, M. Z. Zgierski, P. M. Kozlowski, *Chem. Phys. Lett.* **2000**, *331*, 509.
[50] K. P. Jensen, K. V. Mikkelsen, *Inorg. Chim. Acta* **2001**, *323*, 5.
[51] K. P. Jensen, U. Ryde, *J. Mol. Struct. Theochem*. **2002**, *585*, 239.
[52] K. P. Jensen, S. P. A. Sauer, T. Liljefors, P.-O. Norrby, *Organometallics* **2001**, *20*, 550.
[53] N. Dölker, F. Maseras, A. Lledos, *J. Phys. Chem. B* **2001**, *105*, 7564.
[54] T. Andruniow, M. Z. Zgierski, P. M. Kozlowski, *J. Am. Chem. Soc*. **2001**, *123*, 2679.
[55] K. P. Jensen, U. Ryde, *J. Am. Chem. Soc*. **2003**, *125*, 13970.
[56] P. W. Kozlowski, *J. Phys. Chem. B* **2004**, *108*, 14163.
[57] T. Andruniow, J. Kuta, M. Z. Zgiersky, P. M. Kozlowski, *Chem. Phys. Lett*. **2005**, *410*, 410.
[58] K. P. Jensen, U. Ryde, *J. Am. Chem. Soc*. **2005**, *127*, 9117.
[59] P. M. Kozlowski, T. Kamachi, T. Toraya, K. Yoshizawa, *Angew. Chem. Int. Ed.* **2006**, ASAP.
[60] A. J. Brooks, M. Vlasie, R. Banerjee, T. C. Brunold, *J. Am. Chem. Soc.* **2004**, *126*, 8167.
[61] N. Dölker, F. Maseras, A. Lledos, *J. Phys. Chem.* B **2003**, *107*, 306.
[62] D. Rutkowska-Zbik, M. Jaworska, M. Witko, *Struct. Chem*. **2004**, *15*, 431.
[63] K. P. Jensen, U. Ryde, *ChemBioChem* **2003**, *4*, 413.
[64] M. Jaworska, G. Kazibut, P. Lodowski, *J. Phys. Chem. A* **2003**, *107*, 1339.
[65] T. Wondimagegn, A. Ghosh *J. Am. Chem. Soc.,* **2000**, *122*, 6375.
[66] K. P. Jensen, U. Ryde, *J. Porph. Phtalocyan*. **2005**, *9*, 581.
[67] A. Ghosh, T. Wondimageng, H. Ryeng, *Curr. Opin. Chem. Biol*. **2001**, *5*, 744.
[68] V. Pelmenschikov, P. E. M. Siegbahn, *J. Biol. Inorg. Chem*. **2003**, *8*, 653.
[69] J. L. Craft, Y. C. Horng, S. W. Ragsdale, T. C. Brunold, *J. Biol. Inorg. Chem*. **2004**, *9*, 77.
[70] D. Sundholm, *Phys. Chem. Chem. Phys*. **2003**, *5*, 4265.
[71] A. Pandey, S. N. Datta, *J. Phys. Chem.B* **2005**, *109*, 9066.
[72] M. D. Elkin, O. D. Ziganshina, K. V. Berezin, V. V. Nechaev, *J. Struct. Chem*. **2004**, *45*, 1086.
[73] A. Wong, R. Ida, X. Mo, Z. H. Gan, J. Poh, G. Wu, *J. Phys. Chem. A* **2006**, *110*, 10084.
[74] E. Sigfridsson, U. Ryde, *J. Biol. Inorg. Chem.* **2003**, *8*, 273.
[75] B. Honig, *Science* **1995**, *268*, 1144.
[76] A. J. Mulholland, in Theoretical and Computational Chemistry, Vol. 9, L. A. Eriksson, ed., Elsevier Science, Amsterdam, 2001, pp. 597-653.
[77] U. Ryde *Curr. Opin. Chem. Biol*., **2003**, *7*, 136-142.
[78] N. Källrot, K. Nilsson, T. Rasmussen & U. Ryde *Intern. J. Quant. Chem.,* **2005**, *102*, 520-541
[79] T. H. Rod & U. Ryde, *Phys. Rev. Lett.* **2005**, *94*, 138302.
[80] T. H. Rod & U. Ryde, *J. Chem. Theory Comput*. **2005**, *1*, 1240.
[81] J. M. Pratt, *Pure & Applied Chemistry* **1993**, *65*, 1513.
[82] R. J. P. Williams, *J. Mol. Catal.* **1985**, *30*, 1.
[83] J. Halpern*, Science* **1985**, *227*, 869.
[84] W. R. Scheidt, C. A. Reed, *Chem. Rev.* **1981**, *81*, 543.
[85] J. J. R. Frausto da Silva, R. J. P. Williams, *The biological chemistry of the elements*, Clarendon Press, Oxford, **1994**, p. 10.
[86] R. J. P. Williams, *J. Mol. Catal.* **1985**, *30*, 1.
[87] K. P. Jensen, U. Ryde, *Mol. Phys*. **2003**, *13*, 2003.

[88] A. M. Stolzenberg, M. T. Stershic, *J. Am. Chem. Soc*. **1988**, *110*, 6391.
[89] R. H. Holm, P. Kennepohl, E. I. Solomon, *Chem. Rev*. **1996**, *96*, 2239.
[90] R. A. Marcus, N. Sutin, *Biochim. Biophys. Acta* **1985**, *811*, 265.
[91] B. Kräutler, in: R. B. King (Eds.): *Encyclopedia of Inorganic Chemistry*, John Wiley & Sons, Chichester, England, **1994**, vol 2, p. 697.
[92] M. L. Ludwig, R. G. Matthews, *Annu. Rev. Biochem*. **1997**, *66*, 269.
[93] W. G. Grabarse, F. Mahlert, S. Shima, R. K. Thauer, U. Ermler, *J. Mol. Biol*. **2000**, *303*, 329.
[94] H. L. Schubert, E. Raux, A. A. Brindley, H. K. Leech, K. S. Wilson, C. P. Hill, M. J. Warren, *EMBO J*. **2002**, *21*, 2068.
[95] Y. Shen, U. Ryde, *Chem. Eur. J*. **2005**, *11*, 1549.
[96] H. A. O. Hill, J. M. Pratt, R. P. J. Williams, *Chem. Brit*. **1969**, *5*, 169.
[97] J. H. Grate, G. N. Schrauzer, *J. Am. Chem. Soc*. **1979**, *101*, 4601.
[98] Z. Gross, *J. Biol. Inorg. Chem*. **1996**, *1*, 368.
[99] R. G. Finke, in: B Kräutler, D Arigoni, BT Golding, eds. *Vitamin B_{12} and the B_{12} proteins*, Wiley-VCH, Weinheim, **1998**. Chapter 25.
[100] B. P. Hay, R. G. Finke, *J. Am. Chem. Soc*. **1986**, *108*, 4820.
[101] K. L. Brown, X. Zou, *J. Inorg. Biochem*. **1999**, *77*, 185.
[102] R. G. Finke, B. P. Hay, *Inorg. Chem*. **1984**, *23*, 3041.
[103] R. Padmakumar, R. Padmakumar, R. Banerjee, *Biochemistry* **1997**, *36*, 3713.
[104] S. Chowdhury, R. Banerjee, *Biochemistry* **2000**, *39*, 7998.
[105] S. S. Licht, C. C. Lawrence, J. Stubbe, *Biochemistry* **1999**, *38*, 1234.
[106] R. Banerjee, *Chem. Rev*. **2003**, *103*, 2083.
[107] C. L. Drennan, R. G. Matthews, M. L. Ludwig, *Curr. Opin. Struct. Biol*. **1994**, *4*, 919.
[108] F. Mancia, P. Evans, F. Mancia, N. H. Keep, A. Nakagawa, P. F. Leadlay, S. McSweeney, B. Rasmussen, P. Bösecke, O. Diat, P. R. Evans, *Structure* **1996**, *4*, 339.
[109] K. L. Brown, S. Cheng, X. Zou, J. Li, G. Chen, E. J. Valente, J. D. Zubkowski, H. M. Marques, *Biochemistry* **1998**, *37*, 9704.
[110] H. P. Chen, E. N. G. Marsh, *Biochemistry* **1997**, *36*, 7884.
[111] M. Freindorf, P. M. Kozlowski, *J. Am. Chem. Soc*. 2004, **126**, 1928.
[112] E. N. G. Marsh, *Bioorg. Chem*. **2000**, *28*, 176.
[113] K. Gruber, C. Kratky, *Curr. Opin. Struct. Biol.* **2002**, *6*, 598.
[114] K. Gruber, R. Reitzer, C. Kratky, *Angew. Chem. Int. Ed.* **2001**, *40*, 3377.
[115] F. Mancia, P. R. Evans, *Structure* **1998**, *6*, 711.
[116] N. Dölker, F. Maseras, Siegbahn, P. E. M., *Chem. Phys. Lett*. **2004**, *386*, 174.
[117] R. A. Kwiecien, I. V. Khavrutskii, D. G. Musaev, K. Morokuma, R. Banerjee, P. Paneth, *J. Am. Chem. Soc*. **2006**, *128*, 1287.
[118] K. Peariso, C. W. Goulding, S. Huang, R. G. Matthews, J. E. Penner-Hahn, *J. Am. Chem. Soc.* **1998**, *120*, 8410.
[119] C. L. Drennan, S. Huang, J. T. Drummond, R. G. Matthews, M. L. Ludwig, *Science* **1994**, *266*, 1669.
[120] M. W. Renner, J. Fajer, *J. Biol. Inorg. Chem*. **2001**, *6*, 823.
[121] L. Pauling, C. D. Coryell, *Proc. Natl. Acad. Sci. USA* **1936**, *22,* 210.
[122] G. N. Phillips, Jr, in: A. Messerschmidt, R. Huber, K. Wieghardt, T. Poulos, (Eds.): *Handbook of metalloproteins*, John Wiley & Sons, Chichester, England, 2001.
[123] M. Kotani, *Rev. Mod. Phys.* **1963**, *35*, 717.
[124] K. P. Jensen, B. O. Roos, U. Ryde, *J. Inorg. Biochem*. **2005**, *99*, 45.
[125] T. E. Tsai, J. L. Groves, C. S. Wu, *J. Chem. Phys.* **1981**, *74*, 4306.
[126] H. Eicher, D. Bade, F. Parak, *J. Chem. Phys*. **1976**, *64*, 1446.
[127] H. Eyring, J. Walter, G. E. Kimball, *Quantum Chemistry*, John Wiley & Sons, New York, 1944, p. 330.
[128] M. H. M. Olsson, U. Ryde, B. O. Roos, *Protein Sci.* **1998**, *7*, 2659.

[129] U. Ryde, M. H. M. Olsson, *Intern. J. Quantum. Chem*. **2001**, *81*, 335.
[130] M. H. M. Olsson, U. Ryde, *J. Am. Chem. Soc*. **2001**, *123*, 7866.
[131] E. Sigfridsson, M. H. M. Olsson, U. Ryde, *Inorg. Chem*. **2001**, *40*, 2509.
[132] F. A. Tezcan, J. R. Winkler, H. B. Gray, *J. Am. Chem. Soc.* **1998**, *120*, 13383.
[133] M. L. Fernández, M. A. Martí, A. Crespo, D. A. Estrin, *J. Biol. Inorg. Chem*. **2005**, *10*, 595.
[134] M. Gajhede, in: *Handbook of metalloproteins*, A. Messerschmidt, R. Huber, T. Poulos, K. Wieghart, eds., J. Wiley & Sons, Chicheser, 2001, pp. 285-299.
[135] T. L. Poulos, *Adv. Inorg. Biochem*. **1987**, *7*, 1.
[136] D. Kumar, S. P. de Visser, P. K. Sharma, E. Derat, S. Shaik, *J. Biol. Inorg. Chem.* **2005**, *10*, 181.
[137] Y.-K. Choe, S. Nagase, *J. Comput. Chem*. **2005**, *26*, 1600.
[138] D. Kumar, S. P. de Visser, P. K. Sharma H. Hirao, S. Shaik, *Biochemistry* **2005**, *44*, 8148.
[139] A. Henriksen, A. T. Smith, M. Gajhede, *J. Biol. Chem*. **1999**, *274*, 35005.
[140] T. L. Poulos, *J. Biol. Inorg. Chem*. **1996**, *1*, 356.
[141] D. B. Goodin, *J. Biol. Inorg. Chem*. **1996**, *1*, 360.
[142] L. Capece, M. A. Marti, A. Crespo, F. Doctorovich, D. A. Estrin, *J. Am. Chem. Soc.* **2006**, *128*, 12455.
[143] J. Heimdal, P. Rydberg, U. Ryde, J. Inorg. Biochem., submitted.
[144] B. C. Finzel, T. L. Poulos, J. Kraut, *J. Biol. Chem*. **1984**, *259*, 13027.
[145] U. Ryde, L. Olsen & K. Nilsson, *J. Comput. Chem*. **2002**, *23*, 1058.
[146] U. Ryde, K. Nilsson, *J. Am. Chem. Soc*. **2003**, *125*, 14232.
[147] J. Linnanto, J. Korppi-Tommola, *PhysChemChemPhys* **2006**, *8*, 663.
[148] B. Bobets, I. H. M. van Stokkum, M. Rogner, J. Kruip, E. Schlodder, E. N. V. Karapetyan, J. P. Dekker, R. van Grondelle, *Biophys. J*. **2001**, *81*, 407.
[149] P. Jordan, P. Fromme, H. T. Witt, O. Klukas, W. Saenger, N. Krauss, *Nature* **2001**, *411*, 909.
[150] Y. M. Sun, H. Z. Wang, F. L. Zhao, J. Z. Sun, *Chem. Phys. Lett*. **2004**, *387*, 12.